Morphology of Injection Moulded iPP Samples

R. Pantani, V. Speranza, I. Coccorullo and G. Titomanlio*

University of Salerno – Dept. of Chemical and Food Engineering
Via Ponte don Melillo – I84084 Fisciano (SA) – Italy

Summary: Morphology (in terms of distribution along thickness of crystallinity degree, molecular orientation and dimensions of spherulites) was characterised by adopting different experimental techniques, and analysed with reference to the solidification conditions. Morphological characteristics of the samples were compared with the predictions of a simulation code developed at University of Salerno. In internal layers, calculations provide a satisfactorily description of data. In layers closer to sample skin, results show a large effect of molecular orientation on crystallisation kinetics of alpha phase.

Introduction

Injection moulding process is one of the most widely employed methods for manufacturing polymeric products. During the moulding cycle, the polymer undergoes transitions from fluid to rubbery, and to glassy or crystallised states. It is well known that ultimate physical, optical and mechanical properties of injection mouldings are closely associated with their microstructures[1]. Thus, it is of practical significance to understand the mechanism of microstructure development during the injection moulding of semicrystalline polymers. This is also important for optimising processing variables, such as injection speed, inlet melt temperature, mould temperature, packing pressure and holding time, in an attempt to produce the desired microstructure in the mouldings with the required physical properties. Furthermore, an accurate simulation of the injection moulding process can cut down on the expensive costs of tooling and the trial-and-error mould testing.

It is quite well known that structure development is on its turn influenced by the thermomechanical history[1]. From many experimental observations, it is shown that in injection moulded articles of semicrystalline polymers the high stresses close to the wall give rise to a highly oriented lamellar crystallite microstructure, customarily called the

 CCC 1022-1360/00/$ 17.50+.50/0

skin layer. In the core region, where the stresses are relatively low, the melt is allowed to crystallise three dimensionally to form spherulitic structures. Relative dimensions and morphology of both skin and core layers are dependent on local thermomechanical history. As a result, the skin and the core reveal distinct characteristics across the thickness and along the flow path[1].

Structural and morphological characterisation of the injection moulded polypropylene has received much attention in the past two decades. As early as 1982, Katti and Schultz[2] reviewed the microstructure of injection moulded semicrystalline polymers including polypropylene. The morphology of injection moulded PP tensile bars was extensively studied by Kantz et al. using optical microscopy and X-ray diffraction[3]. Their microscopy results revealed the presence of three distinct crystalline zones: a highly oriented non spherulitic skin with the molecular chains oriented parallellely to the injection direction; a spherulitic shear zone with row or shear-nucleated structure; a spherulitic core with essentially no preferred orientation. Their XRay diffraction studies indicated that the skin layer contains biaxially oriented crystallites due to the biaxial extensional flow. More recently, Fujiyama et al. investigated the skin-core morphology of injection moulded iPP samples using X-ray Small and Wide Angle Scattering techniques[2], and suggested that the shear region exhibits shish-kebab structures. Wenig and Herzog later observed the same shish-kebab structure in the shear region of their moulded samples[3]. A similar investigation was conducted by Titomanlio and co-workers[4], who observed also a high crystallinity degree in the shear zone.

It is rather difficult to theoretically establish the relationship between the observed microstructure and processing conditions. Indeed, a model of the injection moulding process able to predict morphology of final samples is not yet available, even if it would be of enormous strategic importance. This is mainly because a complete understanding of crystallisation kinetics in process conditions (high cooling rates and pressures, strong and complex flow fields) has not yet been reached.

In this work, injection moulding tests were performed using an isotactic polypropylene,

previously characterised as far as most of properties of interest. The resulting morphology of the mouldings (in terms of distribution along thickness of crystallinity degree, molecular orientation and crystals structure and dimensions) was characterised by adopting different experimental techniques, and analysed with reference to the solidification conditions. Morphological characteristics of the samples were compared with the predictions of a simulation code developed at University of Salerno, which implements procedures able to model molecular orientation, crystallisation kinetics and morphology evolution.

Material

A commercial grade iPP resin (T30G, Mw=481000, Mn=75000, tacticity=87.6%mmmm), kindly supplied by Montell (Ferrara, Italy), was adopted for the experiments in this work.

Viscosity

Shear viscosity curves of the material were determined by means of rotational and capillary rheometers operated in the temperature and shear rate ranges 453÷503K and 0.1÷10000 s-1, respectively [5]. All data are well described by the following modified form of the Cross-WLF model:

$$\eta(\dot{\gamma},T,P)=\frac{\eta_0(T,P)}{1+C(\eta_0(T,P)\dot{\gamma})^{1-a}}\ h_\chi(\chi) \qquad (1)$$

where

$$\eta_0(T,P)=D_1\,10^{-\frac{A_1(T-Tr)}{A_2+T-Tr}} \quad (2) \quad \text{and} \quad T_r=D_2+D_3P \quad (3)$$

values of model parameters were identified analysing viscosity data[5] as n=0.37, A_1=2, A_2=250K, D_1=85000 poise, D_2=503K, τ^*=64732 Pa. The value of 0.17K/Pa was taken for the parameter D_3, according to literature indications [6].

The last term in eq. 1 (h_χ) has been added to the standard formulation of the Cross model to describe the effect of the (overall) crystallinity degree, χ, on viscosity, as indicated in the literature[4]:

$$h_\chi(\chi) = \left[1 + f_1 \exp\left(-\frac{f_2}{\chi^m}\right)\right] \qquad (4)$$

Constants in eq. 4 are $f_1=10^{15}$, $f_2=25$ and $m=0.09$, which describe an increase of one order of magnitude when crystallinity (keeping into account all crystalline phases) reaches a value of about 5%.

Material loss, G", and storage, G', moduli were determined by oscillatory measurements in the temperature and frequency ranges 453÷503K and 0.1÷200 s^{-1}, respectively[7]. These measurements are used to describe material viscoelastic properties of a dumbbell population (see below) according to the procedure reported by Pantani et al. [8].

PVT Description

Material PVT behaviour as a function of temperature, pressure and (overall) crystallinity degree was described as[9]:

$$v(T,P) = \chi v_{0cr}(1+\alpha_{cr}(T-T_0)-\beta_{cr}P) + (1-\chi)v_{0am}(1+\alpha_{am}(T-T_0)-\beta_{am}P) \qquad (5)$$

where T_0=298K, χ is the crystallinity degree (keeping into account all crystalline phases), v_{ocr} is specific volume of a fully crystalline sample (taken as 1.03 cm^3/gr[10] at T_0=298K), v_{oam} is specific volume of a fully amorphous sample (taken as1.2 cm^3/gr[10] at T_0=298K), α is thermal expansion coefficient (α_{cr}= 0.002 K^{-1}, α_{am}=0.0006 K^{-1}), β is compressibility factor ($\beta_{cr}=0.98*10^{-6}$ 1/Pa, $\beta_{am}=9*10^{-5}$ 1/Pa[11]).

Moulding test

A 65tons Penta reciprocating screw injection moulding machine was used for the injection moulding experiments. A nozzle of diameter 2.2 mm and length 40 mm was adopted. The sprue tapered from a diameter of 7 mm to a diameter of 4.7 mm over a length of 80 mm. The runner had a diameter of 8 mm and was 68 mm long. The material was injected into a line gated rectangular cavity of 120x30x2mm^3. Five Kistler piezoelectric pressure transducers, were mounted along the flow path. In particular one transducer was mounted in the injection chamber, one in the runner the others in the cavity 15, 60 and 105mm downstream to the gate. These position will be referred to as

P0, P1, P2, P3 and P4 respectively. Transducers signals were read by a data acquisition system and stored in a computer. For all moulding tests, barrel temperature was held at 503K, the mould was conditioned at 303K, holding pressure was 400bar, holding time 10sec, nominal flow rate during the injection-filling step 15cm^3/s. Experimental pressure curves in the five transducers positions are reported in fig. 1.

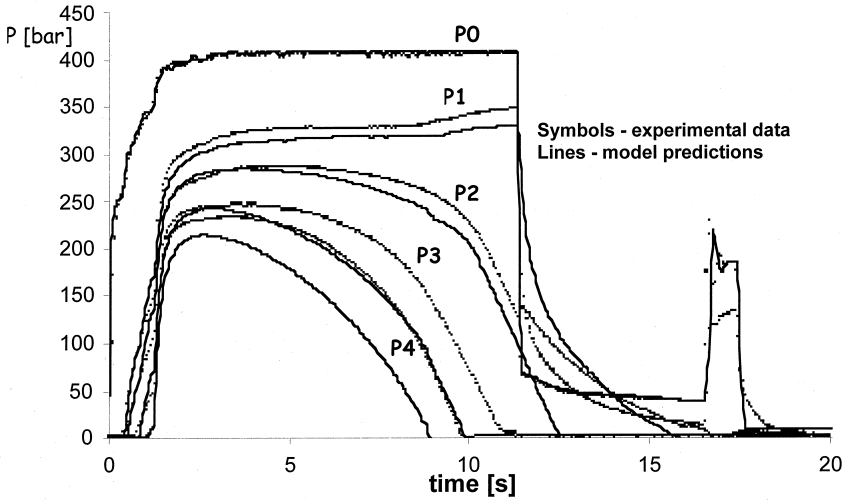

Figure 1. Simulated and experimental pressure curves

Analysis of morphology distribution

Sample Preparation

For crystallinity and morphology investigations, thin slices were cut by means of a Leica slit microtome from moulded samples in the cavity positions where pressure transducers were located. Details of cutting procedures are illustrated in fig. 2: thin slices (about 25μm thick) were cut from the central part of the moulded slab (at pos. P3, central in cavity) along flow (x) direction and parallelely either to the flow-thickness (x,y) plane (scheme A in fig. 2) or to the flow-width (x,z) plane (scheme B in fig. 2). Slices cut according to scheme A refer therefore to a full thickness (=2mm) section of the

sample in pos. P3 (central in cavity) and at 15mm from sample lateral surface. Vice versa, slices cut according to scheme B refer to sections at different distances from sample skin in pos. P3 (central in cavity). All slices were cold lapped soon after cutting procedure.

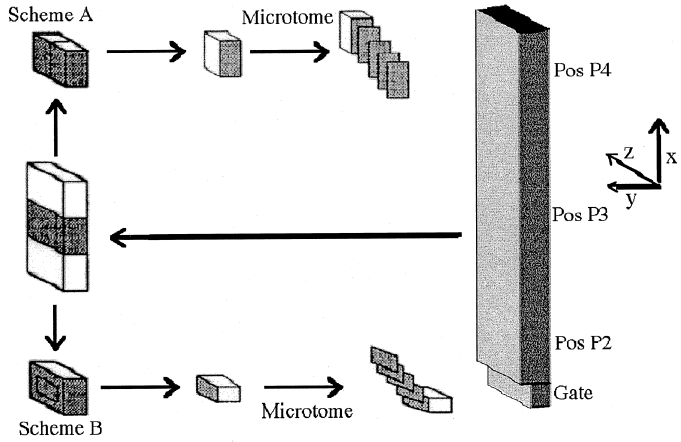

Figure 2. Cutting procedures

Microscopy

In order to gather information on morphology changes with the distance from the sample skin, thin slices, cut from injected samples according to scheme A (flow-thickness plane), were analysed by polarised light optical microscopy. Micrographs are reported in fig. 3 and show a morphology distribution typical of an injection moulded semi-crystalline sample often referred to as skin-core morphology. Micrographs reveal the presence of a series of distinct regions: a thin (about 20μm), slightly oriented, skin layer; a highly oriented non spherulitic zone (the dark zone in fig. 3a, from 20μm to 320μm from skin); a spherulitic core with essentially no preferred orientation.

In order to better characterise skin-core morphology, the same slices were chemically etched according to the procedure suggested by Bassett[12] and then observed using scanning electronic microscopy. Two SEM micrographs are reported in fig. 4: first

micrograph refers to dark zone of fig. 3a (0.1mm from sample skin) and the second one to the central layer (sample midplane).

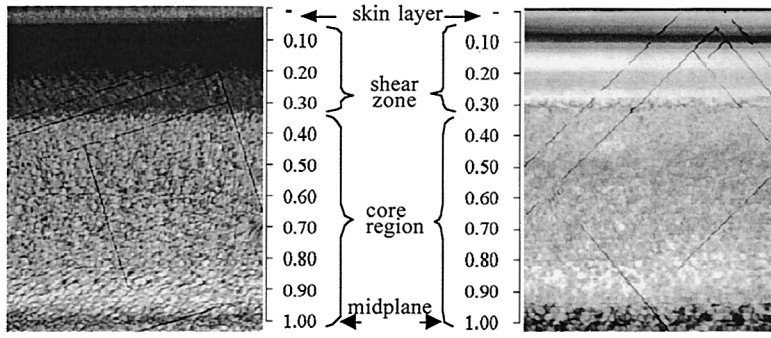

Figure 3. Micrographs in polarised optical light. a) flow direction corresponds to polarizer direction. b) flow direction at 45° with respect to polarizer direction

SEM observations confirm results obtained by optical microscopy: internal layers resulted to be fully spherulitic whereas inside of the dark zone of fig. 3a highly oriented structures (fibers) were observed and no spherulites could be detected. Spherulites diameter was about 20 microns at the internal layer position where SEM observation was performed.

Micrographs (obtained both by SEM and polarized ligth microscopy) were used to evaluate distribution of spherulites diameter along thickness: diameters of spherulites versus distance from the skin are reported in fig. 5 (symbols): biggest spherulites are in the core region and became smaller and smaller from the core region toward the skin.

Birefringence

Birefringence is one of the most sensitive techniques for the measurement of molecular orientation distributions in injection-moulded polymer parts[13]. Indeed measured birefringence value is made of several terms including form and thermal stresses contributions. Form birefringence can be neglected for iPP[14] whereas it can reasonably assumed that after the cutting and surface lapping, all thermal stresses inside the slices

relax. Therefore only contributions due to orientation-induced birefringence of amorphous and crystalline part have been taken into account in this work.

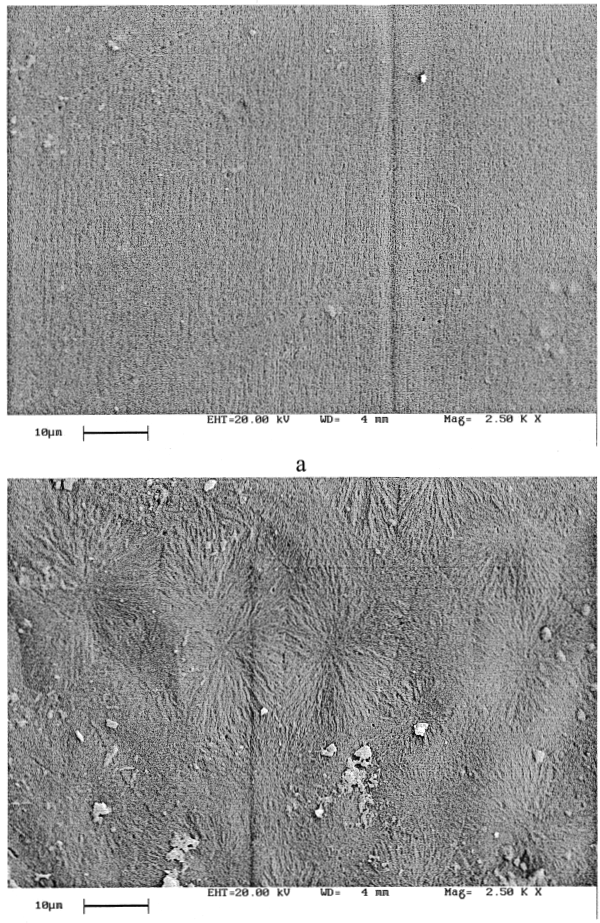

Figure 4. SEM micrographs: a)-skin layer, 100µm from skin, b)-core region, midplane

Birefringence measurements were carried out by scanning with a polarizing microscope the slices cut according to scheme A, moving the objective from skin to the sample midplane. The measuring spot was about 100µm in diameter. At positions closer to sample skin (0÷0.2 mm from the skin), in order to improve spatial resolution, slices

obtained according to scheme B were analysed. Results of birefringence measurements (reported in fig. 6) show that the highest values are reached in correspondence of the dark band of fig. 3a. Even if birefringence is highly influenced by crystallinity, it can be considered an indicator of average (over crystalline and amorphous phases) molecular orientation. Results reported in fig. 6 thus reveal that a peak in average molecular orientation is present in correspondence to the dark zone of fig. 3a.

Birefringence measurements also provide information about the average direction of molecular orientation, as the angle with respect to the flow direction, where a minimum of light intensity passes through crossed polarizers. Distribution along thickness of the angle between direction of molecular orientation and flow direction is reported in fig. 7 (symbols): this angle is smaller in layers close to the wall (about 5°) where orientation is higher, than in layers at the sample core (about 20°).

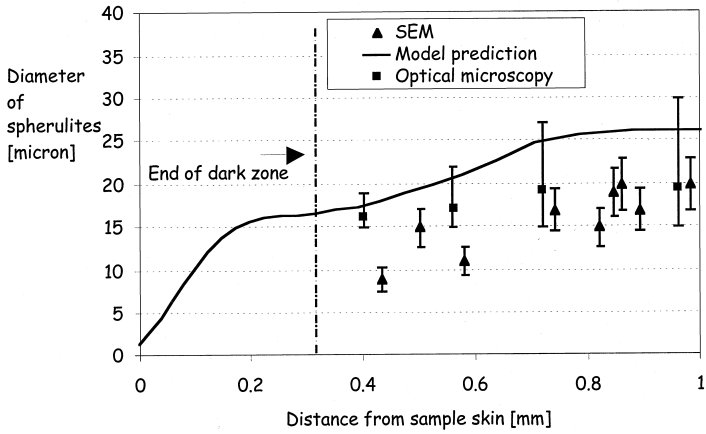

Figure 5. Average diameter distribution along thickness

FTIR Analysis

Slices microtomed from injected samples parallelely to the sample skin (Scheme B) were analysed by means of an IR spectrophotometer (Brucker device), measuring the absorbance in a range from 400 to 4000 cm^{-1}. Crystallinity degree is linked to absorbance

spectrum by the following equation[14]:

$$\chi = \frac{A_{cr}}{A_{cr} + A_{am}\frac{a_{cr}}{a_{am}}} \quad (5)$$

where A_i are absorbances, a_i are the absorption coefficients and the subscripts "am" and "cr" refer to amorphous and crystalline phases, respectively.

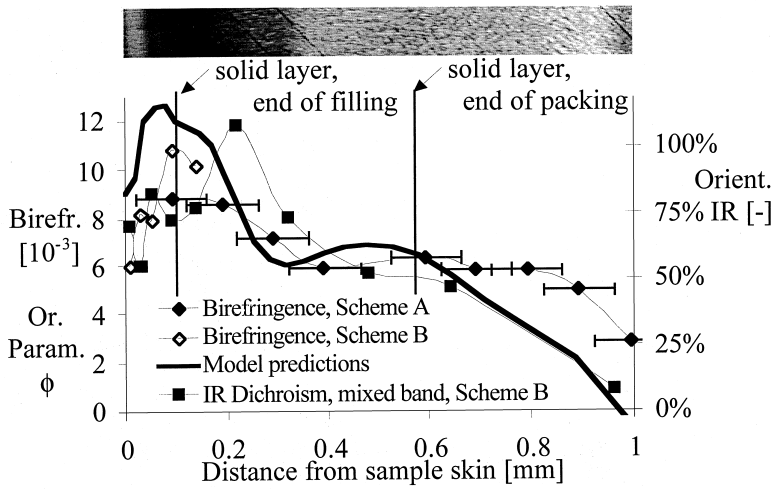

Figure 6. Orientation distribution along thickness as determined by birefringence and by analysis of IR spectra. Results of simulations are also shown (full lines)

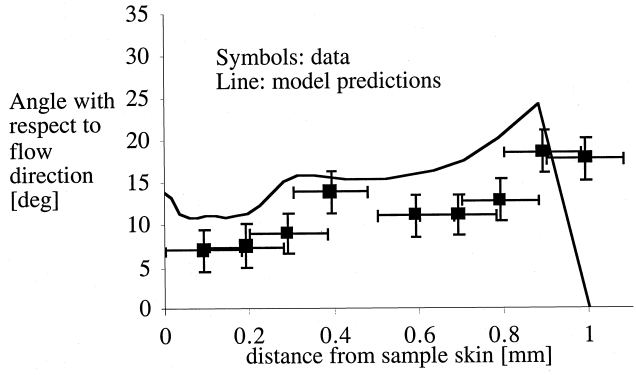

Figure 7. Experimental (symbols) and simulated (full line) distribution along thickness of the angle of average molecular orientation with respect to flow direction

FTIR analysis does not allow to distinguish between different crystalline phases and thus the crystallinity degree as measured by eq. 5 has to be considered as an overall value accounting for all existing crystalline phases. In this work, according to literature indications[14], the bands at 841 cm^{-1} and at 973 cm^{-1} were chosen for crystalline phase and for amorphous phase, respectively. With this bands the ratio of adsorption coefficients (a_{cr}/a_{am}) was calculated as 0.58 by calibration with density measurements. A deconvolution technique was then applied to IR absorption spectra to describe absorption peaks. Results of crystallinity distribution along thickness, calculated by eq. 5, are reported in fig. 8 (symbols) and surprisingly they show that the final average crystallinity degree is about constant along thickness, in spite of the very high cooling rates experienced by the polymer close to sample skin.

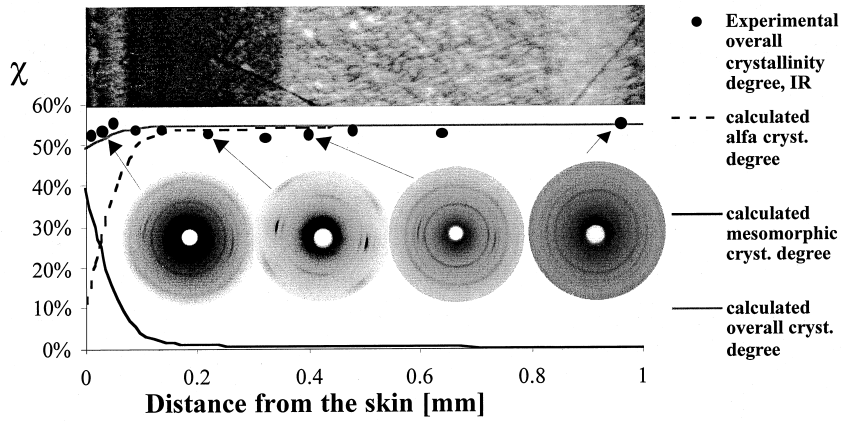

Figure 8. Crystallinity distribution along thickness.

IR spectroscopy is also a very useful technique for the assessment of chain orientation. According to the hypothesis of uniaxial orientation the orientation parameter (Hermann's factor) can be evaluated as[14]:

$$f = \frac{(D-1)(D_0+2)}{(D+2)(D_0-1)}$$

where D is the dicroic ratio, calculated as the ratio between the absorbances of the infrared radiations polarised parallel and perpendicular to the direction of orientation, and D_0 is the dicroic ratio for a sample with perfect uniaxial orientation.

There are some infrared absorption bands that are characterised by absorption by both the crystalline and the amorphous phases. The 1256 cm^{-1} band of isotactic polypropylene is just such a mixed band (for the 1256 cm^{-1} band, D_0 in eq. 6 should be about 3.1610[14]). Results for the mixed amorphous-crystalline orientation are reported in fig. 6 and, even if values are excessively high, they show a qualitative agreement with results of birefringence measurements, confirming a highly oriented zone in correspondence of the dark zone of fig. 3a.

WAXD Analysis

As mentioned above, crystallinity degree measured by IR is an average between α and mesomorphic phases. In order to measure the relative amount of the phases present (α phase, mesomorphic phase and amorphous phase), some of the thin slices cut according to scheme B (flow-width plane) were analysed by WAXD. Some WAXD patterns are reported in fig. 8 and show that average crystallinity in the samples appears to be essentially in the α monoclinic form in most of the sample cross sections.

Modeling

The data of pressure evolution during the process and distributions of final crystallinity, molecular orientation and spherulite diameters have been simulated using the software code developed at University of Salerno, which is based on Lord and Williams model and its extensions[4]. Axial convection, transverse conduction and heat generation, both viscous and due to heat of crystallisation, are kept into account in the energy balance, together with the accumulation term. Lubrication approximation is adopted for the momentum balance. Complex geometries are obtained combining (in series or parallel) simple cylindrical and rectangular elements. Knowledge of inlet injection temperature, zero heat flux at symmetry axis and heat transfer coefficient at mould wall as a function of time are assumed as thermal boundary conditions. Further details about the model can

be found elsewhere [4, 8]

Quiescent Crystallisation Kinetics

Crystallisation model described by Titomanlio and co-workers[15] was adopted in the simulation code. This model is able to satisfactorily describe morphological characteristics of samples solidified under quiescent conditions in a very wide range of cooling rates (up to several hundreds of K/s). It assumes a multiphase picture of the process where the growth of each crystalline phase is governed by individual kinetic functions. Each phase grows independently over the others, but they interact through the competition for the residual amorphous volume. According to this model crystallinity evolution for each form can be expressed as:

$$\frac{d\xi_i(t)}{dt} = \left(1 - \sum_i \xi_i(t)\right) \frac{dk_i(t)}{dt} \qquad (7)$$

where the subscript i stands for a particular crystalline phase (either for α or meso in this work), ξ_i is χ_i/χ_{eqi}, χ_{eq} being the equilibrium crystallinity value, and k_i is the expectancy of crystallised volume fraction of each phase if no impingement would occur.

The evolution of the α crystalline form was described by Kolmogoroff's equation:

$$k_\alpha(t) = \frac{4\pi}{3} \int_0^t \frac{dN[T(s)]}{ds} \cdot \left[\int_s^t G(T(u))du\right]^3 ds \qquad (8)$$

where N(T) is nucleation density and G(T) is the growth rate of the spherulites, both of them being function of T only. According to experimental determinations[15], temperature dependences of nucleation density and growth rate in equation **8** were described by the equations:

$$G[T(t)] = G_0 \exp\left[-\frac{U}{R \cdot (T(t) - T_\infty)}\right] \exp\left[-\frac{K_g \cdot (T(t) + T_m)}{2T(t)^2 \cdot (T_m - T(t))}\right] \qquad (9)$$

$$N(T(t)) = N_0 \exp[\beta \cdot (T_m - T(t))]$$

As mentioned above, according to the model, mesomorphic phase competes with α form for the available amorphous. Mesomorhic phase is assumed to be isokinetic, and

Nakamura kinetic equation was adopted for the expectancy of crystallised volume of mesomorphic phase, k_{meso}:

$$k_{meso} = \ln 2 \left[\int_0^t A(T(s))ds \right]^n \quad (10) \qquad \text{with} \qquad A(T) = K_0 \exp\left[-4\ln 2 \frac{(T - T_{max})^2}{D^2} \right] \quad (11)$$

where n is the Avrami index and A(T) is the kinetic constant, simply expressed by a Gaussian shaped curve (equation 11).

The average final radius of the α spherulites, can be calculated from the final number of nuclei per unit volume, N_a [16]:

$$N_a(t) = \int_0^t \frac{dN[T(s)]}{ds}(1 - \xi(s))ds \quad (12) \qquad \text{obtaining} \qquad R = 3\sqrt{\frac{3\xi_{\alpha final}}{4\pi N_{afinal}}} \quad (13)$$

Parameters used in this work were found[15] by analysing data of quiescent crystallisation as: N_0=17.4 10^{12} nuclei/μm^3, β=0.155, K_g=534858, G_0=2.1 10^{12} μm/s, T_∞=236K, $\chi_{eq\alpha}$=0.55, χ_{eqmeso}=0.44, n=2.83, T_{max}=318K, D=38.3K, U/R=755 K, K_0=4.4 s^{-1}.

Molecular Orientation

The software code adopted for calculation allows to calculate the evolution of molecular orientation by applying simple dumbbell models on the basis of kinematics obtained by a viscous approach [4, 8].

The constitutive equation for elastic dumbbells can be written as

$$\frac{D}{Dt}\underline{\underline{A}} - \underline{\underline{\nabla v}}^T \cdot \underline{\underline{A}} - \underline{\underline{A}} \cdot \underline{\underline{\nabla v}} = -\frac{1}{\tau}\underline{\underline{A}} + \underline{\underline{\nabla v}} + \underline{\underline{\nabla v}}^T \quad (14)$$

where

$$\underline{\underline{A}} = 3\left(\langle \underline{R}\,\underline{R} \rangle - \langle \underline{R}\,\underline{R} \rangle_0 \right) \Big/ \langle R_0^2 \rangle \quad (15)$$

is a measure of the "deformation" of a dumbbell population with respect to the equilibrium state, $\underline{R}$ being the end-to-end vector of a single dumbbell, and the symbol <> determines the average over the configuration space. The maximum eigenvalue of the second order tensor $\underline{\underline{A}}$, referred to as ϕ in the following, was used in this work as an

index of molecular orientation, directly proportional to birefringence. The eigenvector corresponding to ϕ, $\underline{v}_{\phi}$ was adopted to identify the average molecular direction. Once velocity field is known, equation 14 presents a single parameter, the relaxation time, τ, which in this work was allowed to be function of shear rate, temperature and pressure, according to the equations

$$\tau_0(T,P) = \tau^* 10^{\frac{-A_1(T-T_r)}{A_2+T-T_r} h_\chi} \qquad (16)$$

$$\tau(T,P,\dot{\gamma}) = \frac{\tau_0(T,P)}{1+\left[\frac{\tau_0(T,P)\dot{\gamma}}{k}\right]^{1-n}} \qquad (17)$$

Parameters in equations 16 and 17 were determined as a best fitting of data of relaxation time as obtained by oscillatory measurements, according to the procedure described elsewhere [8]. Parameters A_1 and A_2 are the same as in eq. 2, Tr is expressed by eq. 3, h_χ is given by eq. 4, n, τ^* and k were found as 0.233, 7.15s and 0.211, respectively.

Simulation results and discussion

Moulding tests have been simulated using the software code developed at University of Salerno, which is based on the model described above. Nozzle, sprue, runner, gate and cavity were represented by a series of cylindrical and rectangular elements, each of them being divided into a number of rectangular cells (ranging from 50 to 300) in length-thickness (or radii) plane. Thinner cells were taken close to mould wall, were gradients are larger. Finite-differences methods were adopted to solve the equations. Viscosity and material density were described by equations 1 to 5, respectively. Crystallisation kinetics and evolution of the conformation tensor $\underline{\underline{A}}$ were described using the model described above.

Pressure Curves

Simulated and experimental pressure curves for all transducers are reported in fig. 1. Results show that pressure evolution was satisfactorily described at all transducer positions. This was taken as a further confirmation that the code developed at University of Salerno well describes all relevant features of thermomechanical history experienced by the polymer during the moulding tests.

Molecular Orientation

Comparison between experimental distribution of molecular orientation along thickness direction in pos. P3 and model predictions is shown in fig. 6. Results well predict a highly oriented zone in correspondence of the dark band of fig. 3a with a pronounced maximum in correspondence of the layers which solidify during filling (solidification condition being identified when overall crystallinity degree reaches 5%).

The angle which the eigenvector of the tensor $\underline{\underline{A}}$, $\underline{v}_{\phi}$, forms with respect to the flow direction, x, is compared in fig. 7 with the angle of molecular orientation as determined by polarized light measurements. Predictions nicely describe experimental distribution along thickness of the angle between average molecular direction and flow direction.

Crystallinity Distribution

A comparison between experimental data of relative amount of the phases present and model predictions is considered in fig. 8. Predictions of overall (α and mesomorphic phases) crystallinity degree nicely compare with experimental results as measured by IR: overall final crystallinity degree is about constant along thickness, in spite of the very high cooling rates experienced by the polymer close to sample skin. However, as revealed by X-Ray analysis, final crystallinity is mostly in the α form, also close to sample skin, whereas quiescent crystallisation model predicts a prevalence of mesomorphic form at sample skin. Since moulded samples also show a very high degree of orientation at sample skin, it can reasonably be assumed, on the basis of data shown in figures 6 and 8, that this discrepancy is due to the fact that orientation induces an enhancement of crystallisation kinetics of α phase, which develops also in the skin layers (where high cooling rates are present) where the quiescent model for crystallisation predicts the presence of mesomorphic phase. As a consequence, reliable descriptions of microstructure development during injection moulding passes through a deep understanding and a modelling of molecular orientation.

Average Spherulites Diameter Distribution along Thickness

Experimental average spherulites diameter distribution along thickness is compared with model predictions in fig. 5.

Description of data is satisfactory in internal layers; of course the (quiescent) crystallisation model predicts the presence of spherulites also in the dark zone, where SEM analysis revealed that spherulitic structures are replaced by fibers.

Conclusions

Some injection moulding tests were performed using a commercial grade isotactic polypropylene. Sample final morphology was characterised in terms of distribution along thickness of crystallinity degree, molecular orientation and dimensions of spherulites by means of several experimental techniques.

Final morphological characteristics of samples were compared with the predictions of a simulation code developed at University of Salerno for the simulation of the injection moulding process on the basis of quiescent crystallisation kinetics. Calculations provide a satisfactorily description of data in terms of both crystallinity degree and diameter of spherulites in internal layers. In layers closer to sample skin, results show a large effect of molecular orientation, which gives rise to a considerable enhancement of crystallisation kinetics of α phase with respect to quiescent conditions.

A better description of injection moulding can be obtained only after considering the effect of the molecular orientation on crystallisation kinetics.

Acknowledgements

Thanks are due to Augusto Autuori for carrying most of the experiments within his thesis for doctorate in Chemical Engineering. The work is supported by the Italian Ministry of University (PRIN 1999-2001, "Flow induced crystallization of polymers. Impact on processing and manufacturing properties").

[1] Cunha, S. Fakirov, *"Structure Development During Polymer Processing"*, Kluwer Academic Publisher,**1999**.

[2] M. Cakmak, C. M. Hsiung, Y. D. Wang, *"Structure development in injection molding of semicrystalline polymers"*, Shiguma Syuppan Publisher, November **1997**.

[3] X. Guo, A. I. Isayev, I. Guo, *Polym Eng Sci*, **1999,** *39*, 2096
[4] G. Titomanlio, V. Speranza, V. Brucato, *Intern Polym Proc* **1997,** *12*, 45.
[5] N. Grizzuti. Personal communication
[6] M.A. Couch, D.M. Binding, *Polymer* **2000,** *41*, 6323
[7] M.R. Nobile Personal communication
[8] R Pantani, V Speranza, A Sorrentino, G Titomanlio, Proc. of FICOP, Salerno 2001
[9] R. Pantani, V. Speranza, G. Titomanlio, *Intern Polym Proc* **2001** *16*, 61
[10] C.R. Progelhof, Throne J.L. "*Polymer Engineering Principles*", Hanser Publisher, **1993**.
[11] A. Autuori "*Analisi di manufatti polimerici stampati*" Master Thesis (in Italian), Salerno **2001**
[12] H.M. White, D.C. Basset, *Polymer* **1998,** *39*, 3211
[13] Wimberger-Friedl, *Prog Polym Sci* **1995,** *20*, 369
[14] R. J. Samuels, "*Structured Polymer Properties*", John Wiley & Sons, New York, **1974**.
[15] I. Coccorullo, R. Pantani, G. Titomanlio, *Crystallisation Kinetics And Solidified Structure in Polymers under High Cooling Rates,* in preparation
[16] G. Eder, H. Janeschitz-Kriegl, "*Crystallization*" in Material Science and Technology, edited by Han E. H. Meijer, **1997**, vol 18.
[15] I. Coccorullo, R. Pantani, G.C. Alfonso, G. Titomanlio, Proc. of AIM Meeting, Trento 2001.